Research Article

Microtubules Growth Rate Alteration in Human Endothelial Cells

**Irina B. Alieva,[1,2] Evgeny A. Zemskov,[2] Igor I. Kireev,[1] Boris A. Gorshkov,[2]
Dean A. Wiseman,[2] Stephen M. Black,[2] and Alexander D. Verin[2]**

[1] *Electron Microscopy Department, A.N. Belozersky Institute of Physico-Chemical Biology, Moscow State University,
119992 Moscow, Russia*
[2] *Vascular Biology Center, Medical College of Georgia, Augusta, GA 30912, USA*

Correspondence should be addressed to Irina B. Alieva, irina_alieva@belozersky.msu.ru

To understand how microtubules contribute to the dynamic reorganization of the endothelial cell (EC) cytoskeleton, we established an EC model expressing EB3-GFP, a protein that marks microtubule plus-ends. Using this model, we were able to measure microtubule growth rate at the centrosome region and near the cell periphery of a single human EC and in the EC monolayer. We demonstrate that the majority of microtubules in EC are dynamic, the growth rate of their plus-ends is highest in the internal cytoplasm, in the region of the centrosome. Growth rate of microtubule plus-ends decreases from the cell center toward the periphery. Our data suggest the existing mechanism(s) of local regulation of microtubule plus-ends growth in EC. Microtubule growth rate in the internal cytoplasm of EC in the monolayer is lower than that of single EC suggesting the regulatory effect of cell-cell contacts. Centrosomal microtubule growth rate distribution in single EC indicated the presence of two subpopulations of microtubules with "normal" (similar to those in monolayer EC) and "fast" (three times as much) growth rates. Our results indicate functional interactions between cell-cell contacts and microtubules.

1. Introduction

One of key topics in contemporary biology is a dynamic morphology of cells, and endothelial cells (EC), in particular, which is closely related to cooperative dynamics of cytoskeleton and cell adhesive structures. Cell systems participating in this process comprise not only structural components and associated mechanisms (cytoskeleton fibrils, molecular motors, and adhesive receptors), but also regulatory and signaling elements modulating the dynamics and interactions among these structural units.

The primary function of the EC lining the inner surface of all vessels is to regulate permeability of vascular walls and control the exchange between circulating blood and tissue fluids. The EC cytoskeleton plays a crucial role in maintaining endothelial barrier function. Cytoskeleton reorganization changes the cell shape and provides structural basis for an enhancement as well as a loss of endothelial barrier function. Increases in vascular permeability, common for a number of human pathological states and diseases, such as inflammation, asthma, sepsis, acute lung injury,

ischemia, and diabetes, can lead to severe, and even fatal, organ dysfunction [1–6]. Previous studies, published by us and by others, have proved that normal functioning of the endothelial barrier is provided by the balance between contracting and stretching forces generated by cytoskeleton proteins [3, 5, 7–9]. Moreover, endothelial cell-cell adherens junctions (AJs), largely composed of vascular endothelial cadherin (VE-cadherin), are the basic structure of endothelial permeability regulation because of their dynamic ability to open and close [10, 11]. The role of actin cytoskeleton in the formation, maintenance, and functionality of AJs in EC is well characterized [12–14]. However, the potential link between AJs and microtubules has not been well investigated.

As a major component of cytoskeleton, microtubules have important functions in various cellular processes, such as cell shape formation, cell polarization, and motility [15–22]. In many cell types, microtubules are organized in a radial array with their minus-ends anchored at the centrosome and their plus-ends extending toward the cell periphery where they are involved in a number of essential cellular events [23–25]. Microtubules are known to interact with

2

Journal of Biomedicine and Biotechnology

the cell-cell adhesion machinery in fibroblasts [26] and in epithelial cells [27–31]. It was also shown that microtubule dynamics is an important factor in regulation of cell-cell contacts [30–32]. Our previous data demonstrated the critical involvement of the microtubule disassembly in induced EC barrier dysfunction [8, 9, 33] and allowed us to assume that microtubule dynamics is an early event in the circuit of the reactions leading to the changes in pulmonary EC barrier permeability [33]. Here we described a cellular model established in physiologically-relevant human pulmonary artery EC (HPAEC). This model is suitable for real-time study of microtubule organization and dynamics in the quiescent human EC monolayer as well as in the cells treated with the agents compromising/enhancing endothelial barrier. Using this model we were able to obtain several key parameters of microtubule organization in the endothelium such as a ratio between stable and dynamic microtubule subpopulations, direct measurement of microtubule growth rates, and their difference in single EC and the cells grown as a monolayer. In our opinion, this cellular model would also allow us to study the involvement of microtubules in the barrier-protective/compromising mechanisms activated in pulmonary endothelium by various pharmacological agents of interest.

2. Materials and Methods

2.1. Cell Culture. HPAEC were obtained from Clonetics BioWhittaker Inc. (USA) and cultivated in complete EGM-2 medium (Clonetics BioWhittaker) at 37°C in an atmosphere of 5% CO_2. Experiments were performed on cultures at 6–10th passages, seeded at ≈30% confluence, and utilized either at ≈50% confluence or when fully confluent (depending on the type of experiments).

2.2. Antibodies and Immunofluorescence Microscopy. As primary antibodies for microtubule staining, we used monoclonal mouse antibody against β-tubulin (ICN, USA) (1 : 200), monoclonal mouse antibody against acetylated tubulin (Accurate Chemicals, USA) (1 : 100), and monoclonal mouse antibody against tyrosinated tubulin (ICN, USA) (1 : 100). Antimouse antibodies conjugated to the fluorescent dyes Alexa-488 or Alexa-594 (Molecular Probes, USA) (1 : 100) were used as secondary antibodies.

Prior to immunofluorescence staining, HPAEC grown on glass coverslips were fixed for 10 minutes with a 1.5% solution of glutaraldehyde (Sigma, USA) in phosphate-buffered saline (PBS), pH 6.8 (Sigma, USA) and washed 3 times with PBS (each washing session lasted 10 min). Fixed cells were permeabilized with 0.1% Triton X-100 (Sigma, USA) in PBS for 15 minutes and washed thrice with PBS for 10 minutes. To avoid background fluorescence, prior to staining with antibodies the cells were treated with a 0.2% solution of sodium borohydride ($NaBH_4$) (Sigma, USA) in PBS (10 min, three times) and washed 3 times with PBS for 10 minutes. The next step included incubation of cells with primary (30 min, 37°C) and secondary (30 min, 37°C) antibodies. The coverslips were mounted on slides in water/glycerol mixture (1 : 1) as priming medium. Prior to

assays, cover glass edges were sealed with nail polish for better fixation of the samples.

Immunofluorescence stainings of EC monolayers were examined under a Nikon Eclipse TE2000 microscope (Nikon Intech Co., Japan) supplied with a 60/1.4 objective. The most spread cells were selected in order to ensure better visualization of the cell structures. Images were recorded using Hamamatsu ORCA-2 (Hamamatsu Photonics, Japan) digital cooled CCD camera supported with MetaView software (Universal Imaging, USA). The resolution of 12-bit digital images was 9 pixel/μm. Image processing was performed using MetaMorph (Universal Imaging, USA) and Adobe Photoshop 7.0 (Adobe Inc., USA) software.

2.3. Quantitative Analysis of Microtubule Network. Quantitative analysis of microtubules was carried out as described previously and included measurement of their fluorescence using the MetaMorph software and analysis of digital images collected with a digital CCD camera [8, 9]. For the analysis, extended focus images of well-spread cells with minimal thickness were used. Microtubule subpopulations in the area of interest were computed by the original image segmentation with threshold set to 200% of background level and by calculating the percentage of above-the-threshhold pixels. The relative area occupied by the microtubule network in different cell compartments was calculated in three different areas: (1) an area circumjacent to the cell periphery that was 5 μm from the cell margin; (2) an area circumjacent to the cell periphery that was 10 μm from the cell margin; and (3) the inner compartment, that is, the internal cytoplasm (10 μm from the cell margin) not including the first two areas. The ratio between the area occupied by microtubules to the measured area was determined separately for each measured area. Statistical analysis with performed with Sigma Plot 7.1 (SPSS Science, USA) and Excel (Microsoft Corp., USA). Sigma Plot 7.1 software was used for graphical data presentation.

2.4. Expression Construct and Transfection of Plasmid. To calculate the microtubule growth rate in living HPAEC we used previously described expression vectors encoding EB3-GFP (kind gift of Dr. I. Kaverina [Vanderbilt University, Nashville] with permission from Dr. A. Akhmanova [Erasmus University, Rotterdam]), which serves as a marker of growing distal tips (plus-ends) of microtubules [34]. Effectene transfection reagent (Qiagen Inc., USA) was used for transfection of plasmids into HPAEC cells according to the manufacturer's protocol. Transfected cells were selected for imaging by GFP fluorescence.

2.5. Video Microscopy of EB3-GFP-Transfected Cells. For live imaging, the cells were cultured on glass-bottomed dishes with No.1S coverslips (Iwaki, Japan). Images of cells were collected with a PC-based DeltaVision optical sectioning system using PlanApo 100x/1.40 NA oil or PlanApo 60x/1.40 NA oil ph3 objectives (Olympus). Images were acquired with a cooled CCD camera (Hamamatsu Photonics) with an appropriate ND filter, binning of pixels, exposure time, and

time intervals. Fluorescence signals were visualized using the Endow GFP bandpass emission filter set (41017, Chroma) for GFP imaging.

2.6. Video Analysis. Quantitative analysis of the microtubule dynamics was carried out on time-lapse movies of cells expressing EB3-GFP. Microtubule growth rates were obtained by tracking EB3-GFP comets at microtubule plus-ends (1 second/frame) using ImageJ software linked to an Excel spreadsheet. Statistical analysis was performed using Sigma Plot 7.1 (SPSS Science, USA).

3. Results

Previously, we demonstrated that the microtubule population in EC is heterogeneous and partly represented by posttranslationally modified (acetylated) microtubules [8]. Acetylated microtubules are less dynamic than intact tyrosinated microtubules and more resistant to the effects of external factors. Therefore, under conditions compromising vascular endothelium integrity, they may confer stability on the endothelial microtubule network. Moreover, we can assume that some EC barrier-enhancing factors may shift the ratio in favor of stable microtubule subpopulation and increase overall stability of the EC cytoskeleton. Since the ratio of dynamic (tyrosinated) and stable (acetylated) microtubules in EC has not yet been determined, in first set of experiments, we addressed this question using immunofluorescence staining of the modified tubulins followed by visualization and quantification of dynamic and stable subpopulations of microtubules. In our study, we also focused on direct tracking growing distal tips of microtubules (plus-ends) in order to establish an adequate model to study microtubule dynamics in EC monolayers and single cells. We also wanted insights for further analysis of microtubule-dependent response in EC under barrier-compromising/enhancing conditions.

3.1. Dynamic Microtubule Plus-Ends Reach the Cell Periphery in Human EC. Immunofluorescence staining of β-tubulin in human EC revealed that the microtubule network had a well-defined convergent center near the nucleus (Figure 1(a)). The density of the microtubule network was the highest in the internal cytoplasm, but diminished gradually in the direction of the cell margin. Single microtubules were visualized at the cell periphery. On average, microtubules occupied 47.9 ± 4.1% of the total cell area (n = 20) (Figure 1(d)). In the cell interior, the relative area occupied by microtubules was 83.3 ± 5.8% (n = 20). The microtubule population density decreased from the cell center to cell margin. In the area circumjacent to the cell periphery (10 μm from the cell center), microtubules occupied up to 28.3 ± 7.4% of the total cell area. At the cell edge (5 μm from the cell margin), microtubules occupied 15.7±6.6% of the cytoplasm area.

As mentioned above, endothelial microtubule network is heterogeneous, which is consistent with the dynamic characteristics of its constituent microtubules. The microtubule population can be divided into two subpopulations: stable, modified (acetylated), and dynamic (tyrosinated) microtubules.

The subpopulation of stable (acetylated) microtubules was identified by immunofluorescence staining using antibody against acetylated tubulin. In quiescent EC monolayers, acetylated microtubules were predominantly localized in the cell center and were devoid of a well-defined convergence center (Figure 1(b)). Quantitative analysis demonstrated that acetylated microtubules occupied only 17.1 ± 4.3% (n = 20) of the cell surface or ~35% of the total microtubule network area (Figure 1(d)). Acetylated microtubules were practically not detected near the cell margin (Table 1).

The subpopulation of intact tyrosinated microtubules [35] was identified by immunofluorescence staining of EC using antibody against tyrosinated tubulin (Figure 1(c)). The distribution pattern of tyrosinated microtubules was similar to that of the microtubule network immunostained with anti-β-tubulin antibody (Figures 1(a) and 1(c)). This subpopulation had a well-defined convergence center near the nucleus. The density of tyrosinated microtubules diminished from the cell center to the cell margin. Tyrosinated microtubules (n = 20) occupied 47.0 ± 3.6% of the total cell area, which is consistent with the corresponding parameter for the microtubule system in general (Figure 1(d)).

3.2. Microtubule Plus Ends Growth Faster in the Cell Center than Near the Periphery in Human EC. In addition to quantitative analysis of the areas occupied by dynamic and stable microtubules in different compartments of human EC, we calculated microtubule plus-ends growth rates in EC. Two problems have hindered the direct observation of microtubule nucleation at the centrosome region. First, high microtubule density at the centrosome makes it difficult to visualize individual microtubules. Second, the EC are generally thick in the region of the centrosome, which results in substantial out-of-focus fluorescence that degrades imaging of individual fluorescently labeled microtubules. To specifically visualize microtubule growing ends, we used EB3-GFP as a marker of growing distal tips of microtubules [34]. Microtubule growth rates were obtained by tracking EB3-GFP comets at microtubule plus-ends.

We evaluated microtubule growth rates in the central region and near the cell periphery of human EC by tracking individual EB3-GFP dashes as they emerged from the centrosome and grew outwards in the direction of cell periphery (Figure 2). In HPAEC monolayer, the instantaneous rate of microtubule plus-ends growth was the highest at the cell center, in the centrosome region, and it was 25% lower near the cell margin (Figure 3; Table 2). We observed plus-ends growth episodes at a rate exceeded 40 μm/min in the centrosome region but not on the cell periphery.

A portion of microtubule plus-ends grew persistently from the centrosome, reaching the cell edge before the comet of EB3-GFP was lost. In some cases, GFP-labeled growing plus-ends were observed to reach the edge of the cell and continue to grow along the edge. This observation suggests
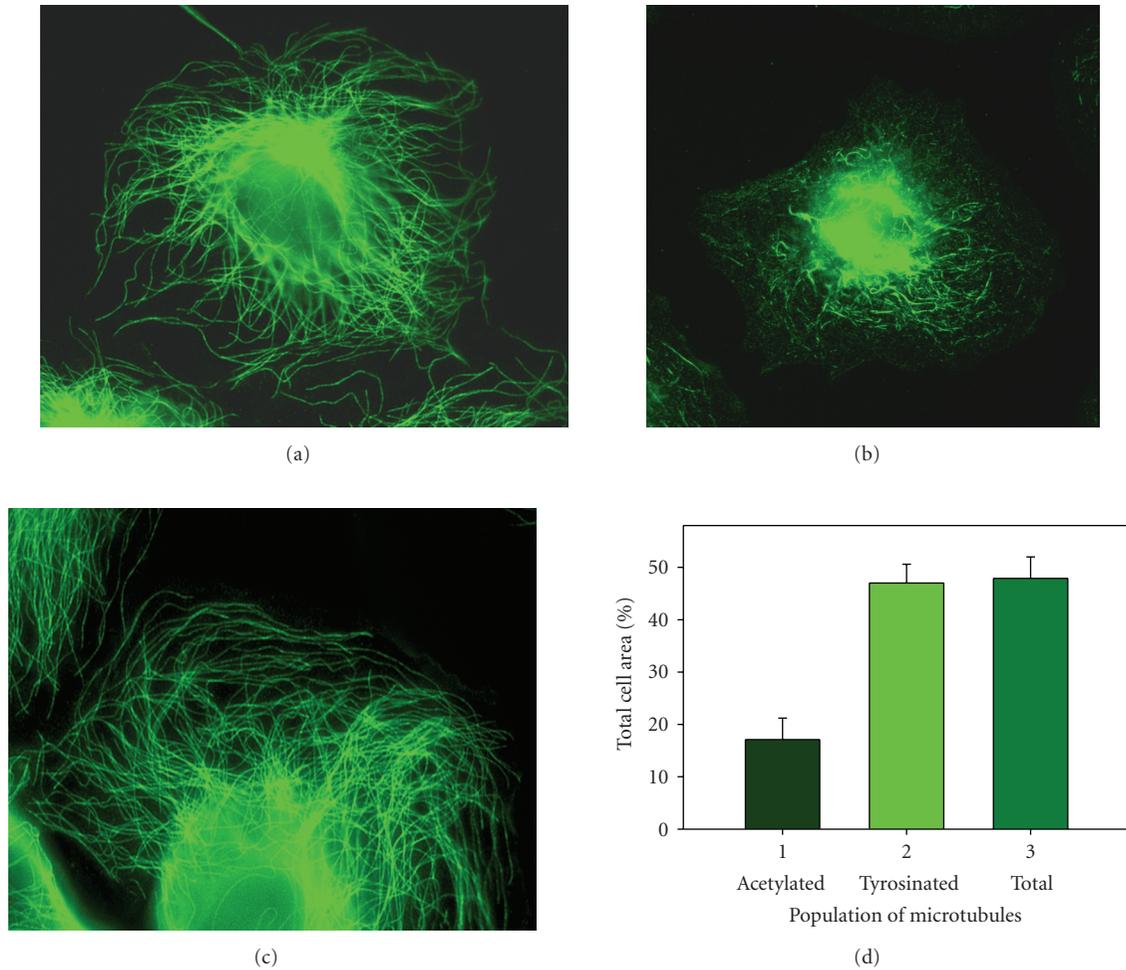
(a)

(b)

(c)

(d)

FIGURE 1: Dynamic microtubules are directed towards and their ends reach the cell periphery. HPAEC were fixed and processed for immunofluorescence microscopy. (a) Antibodies against β-tubulin were used to detect total microtubule population of the cell; (b) antibodies against acetylated tubulin were used to detect stable microtubules; (c) antibodies against tyrosinated tubulin were used to detect dynamic microtubules. Scale bar, $20\,\mu$m; (d) relative area occupied by microtubules (% of the total cell area): *1*—acetylated microtubules; *2*—tyrosinated microtubules; *3*—total population of cell microtubules.

TABLE 1: Quantitative analysis of areas occupied by dynamic and stable microtubules in different compartments of human EC.

| Microtubules of interest | Area occupied by microtubules of interest, % | | |
| | Total cell area | Cell periphery | |
		$10\,\mu$m from the margin	$5\,\mu$m from the margin
β-tubulin stained microtubules	47.9 ± 4.1	$28.3 \pm 7.4^*$	$15.7 \pm 6.6^*$
Acetylated microtubules	17.1 ± 4.3	$2.7 \pm 0.9^*$	$0.4 \pm 0.3^*$
Tyrosinated microtubules	47.0 ± 3.6	Not shown	Not shown

* Significant difference from total cell area at 95% confidence level. Student's *t*-test was used for statistical analysis.

that the cell edge in human EC does not always alter the behavior of the microtubule end, and, at least in some cases, the plus-end can change its trajectory and continue to grow along the cell border. Analysis of growth rates for radially-oriented microtubules and microtubules growing along the cell border showed very similar instantaneous rates of microtubule plus-ends—$12.4 \pm 0.1\,\mu$m/min ($n = 206$) and $11.9 \pm 0.1\,\mu$m/min ($n = 115$), respectively.

3.3. *Microtubule Plus-Ends Growth Rate in the Centrosome Region Is Higher in a Single Cell than in Cells Growing as a Monolayer.* We examined microtubule dynamics in the centrosome region in cells contacted on all sides with neighboring cells (EC monolayer) and in single cells. The results obtained using EC expressing EB3-GFP visually demonstrated that growing microtubule plus-ends were distributed in a relatively uniform manner in a single human
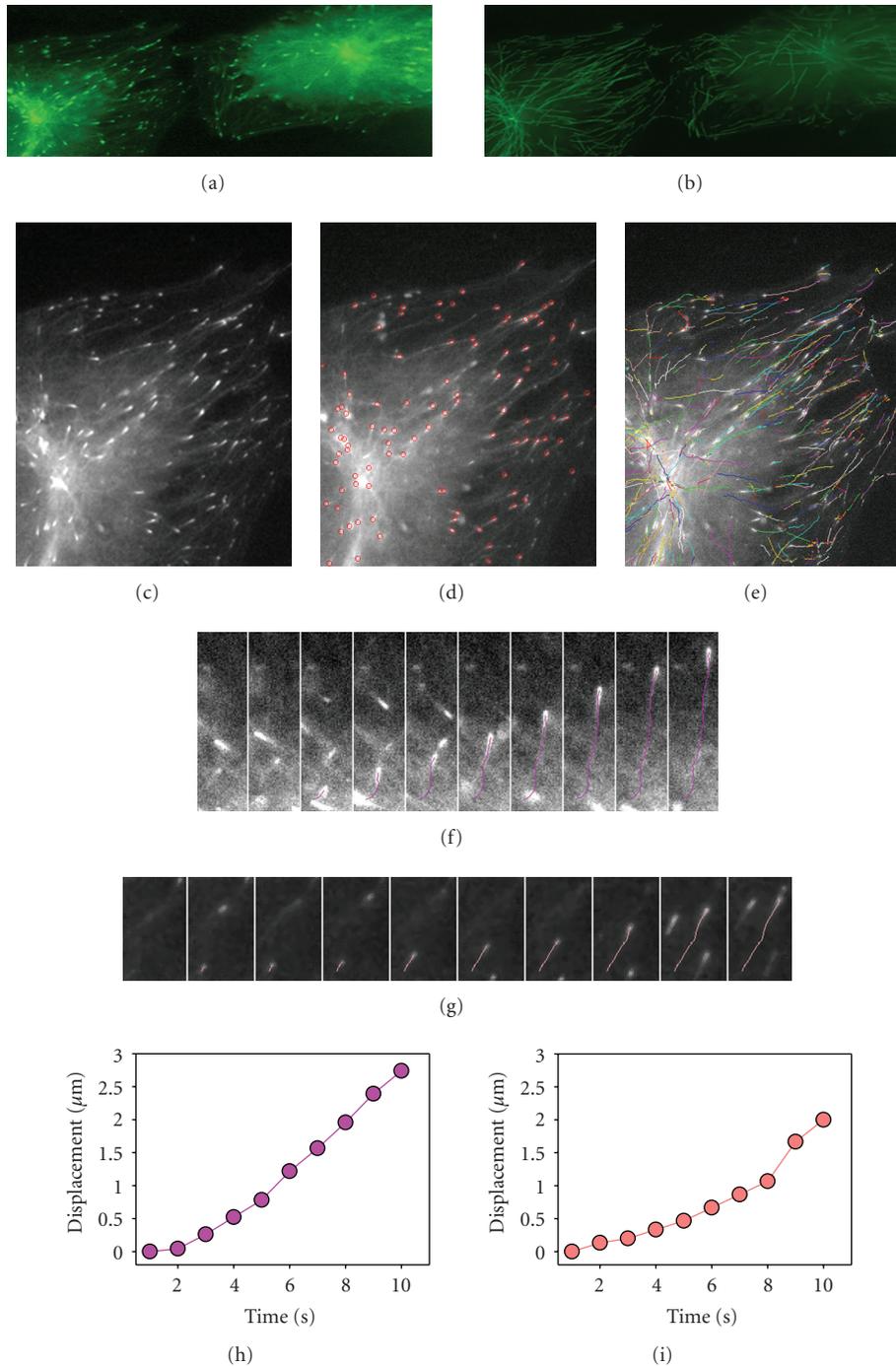
FIGURE 2: Selective visualization of growing microtubule plus-ends in human EC. EB3-GFP was used as a marker of growing distal tips (plus-ends) of microtubules. HPAEC were transfected with the plasmid expressing EB3-GFP and the cells growing in monolayer were selected for analysis. Not all cells in the monolayer expressed the construct, and, therefore, could be detected in the fluorescence micrographs. Persistent microtubule growth was confirmed by long EB3-GFP tracks. EB3-GFP movement was analyzed by time-lapse microscopy. Images were acquired every 1 second. ((a), (b)) Two neighboring EC expressing EB3-GFP, low magnification. (a) EB3-GFP tracks oriented radially from the centrosome can be seen to elongate persistently. EB3-GFP is presented at microtubule plus-ends during growth phases but disappears after transition from growth to pause or shortening phase. (b) EB3 tracks obtained by EB3-GFP patches displacement on time-lapse series during 60 second. Scale bar, $10\,\mu$m. ((c)–(e)) High magnification of left cell from two EB3-GFP expressing EC shown in ((a), (b)): (c) first frame; (d) the same frame with EB3-GFP patches marked with red circles for analysis; (e) EB3 tracks obtained by EB3-GFP patches displacement on time-lapse series during 60 seconds (are colored individually). Scale bar, $10\,\mu$m. ((f), (g)) High magnification of the frames 1–10. (f) Ten consecutive frames (1–10 sec.) showing the movement of EB3-GFP comet on microtubule tip growing radially from the centrosome region. EB3 tracks (purple) obtained by EB3-GFP patches displacement during 10 seconds. (g) EB3 tracks (pink) obtained by EB3-GFP patches displacement during 10 second near the cell margin. (h) Quantification of plus-ends displacement of microtubules shown in (f). (i) Quantification of plus-ends displacement of microtubules shown in (g).

TABLE 2: Microtubule plus ends growth rate in different areas of human EC.

Position	Growth rate* (μm/min)
Centrosome region	16.7 ± 0.3 ($n = 82$)
Cell margin	$12.9 \pm 0.1^{**}$ ($n = 300$)

*Instantaneous rates measured from positions of EB3-GFP dashes in sequential frames of a time-lapse series.
**Significant difference from centrosome region at 95% confidence level. Student's t-test was used for statistical analysis.
n = number of microtubules.

EC as well as in a cell in monolayer where cell-cell contacts, mainly AJs, were formed and well-organized. Quantification of microtubule plus-ends growth rates showed that in single cells the instantaneous rate of microtubule plus ends growing in the centrosome region was $20.6 \pm 0.6\,\mu$m/min ($n = 72$). Comparing this instantaneous rate with that calculated for the monolayer, we concluded that in monolayer-growing cells, the rate of microtubule plus ends growth was 20% lower than in single cell (Figures 2, 3; Table 2).

The histogram of centrosomal microtubules growth rate distribution demonstrated two peaks in single human EC: the first peak showed a correlation with a growth rate near 18–20 μm/min, the second peak of the histogram started with a growth rate more than 32 μm/min and frequency of episodes of fast growth that had a second maximum at 45–50 μm/min. It is possible to explain an origin of the second peak on the microtubule growth rates histogram (Figure 4), based on two assumptions. First, one can assume the existence of two different groups of centrosomal microtubules with various growth rates. From the other side, it is possible that the same individual microtubule can grow quickly for a few frames of the recording and then grow more slowly. However, the analysis of the entire data file of microtubule growth rates measurement (data is not shown) has not revealed sudden fluctuations in growth rates of individual microtubules depending on observation time. The presented representative examples of microtubules plus-ends displacements (Figures 2(f), 2(g), 2(h), and 2(i)) demonstrate that growth rates of individual microtubules does not undergo dramatic changes during observation time.

Therefore, based on data obtained, we could distinguish two different groups of centrosomal microtubules according to their growth rates. Most of microtubules (85% of growth episodes—Figure 4) belonged to the group with "normal" growth rates. Another group of the microtubules (15% of growth episodes—Figure 4) was characterized by fast growth rates. The growth rates in the first group coincided with those characteristic for microtubules in the EC monolayer (average growth rate $14.4 \pm 3.3\,\mu$m/min). Average growth rate in the second ("fast") group was much higher—$59.4 \pm 4.3\,\mu$m/min. Since growth rate of "fast" microtubules was approximately three times higher, their contribution to average growth rate was quite significant. Our results suggest that in the population of single cells, the average growth rate was about 20% higher than the growth rate of microtubules polymerizing in the EC monolayer.
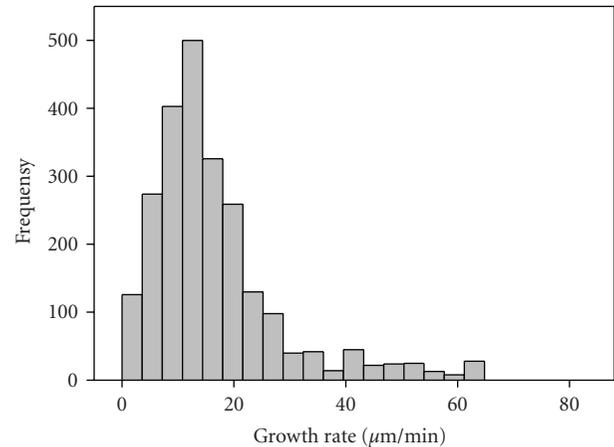
(a)
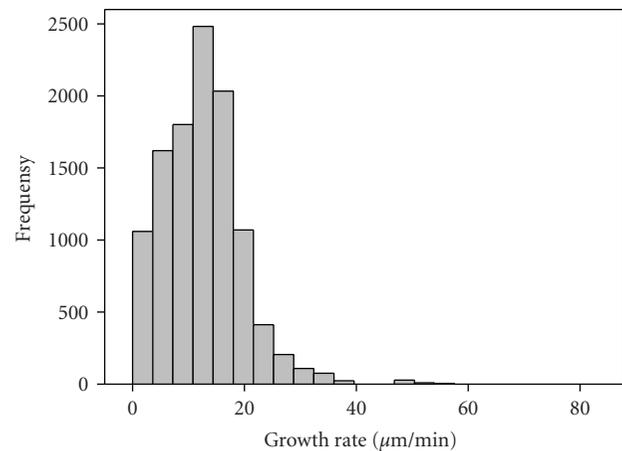
(b)

FIGURE 3: Microtubule plus-ends growth rates are different in centrosome region and on the periphery near the cell margin. Growing microtubule plus-ends were selectively marked in human EC. HPAEC were transfected with the plasmid expressing EB3-GFP. Persistent microtubule growth was confirmed by long EB3-GFP tracks. EB3-GFP movement was analyzed by time-lapse microscopy. Images were acquired every 1 second. Histogram of microtubule growth rate distribution were obtained by tracking EB3-GFP comets at microtubule plus-ends in HPAEC in the centrosome region (mean growth rate, $16.7 \pm 0.3\,\mu$m/min ($n = 82$)) (a) and near the cell margin (mean growth rate, $12.9 \pm 0.1\,\mu$m/min ($n = 300$)) (b).

By analyzing the local microtubule dynamics in the internal cytoplasm and near the cell margin in human EC, we have found that the microtubule plus-ends growth rate on the cell periphery (near the cell margin) is lower than in the internal cytoplasm. We could also conclude that the growth rate on the periphery did not depend on microtubule tips growth orientation along or perpendicular to the cell border. We can speculate that microtubule growth rate closely depended on AJs availability, and it is lower in monolayer-growing EC where cell-cell contacts were fully formed.
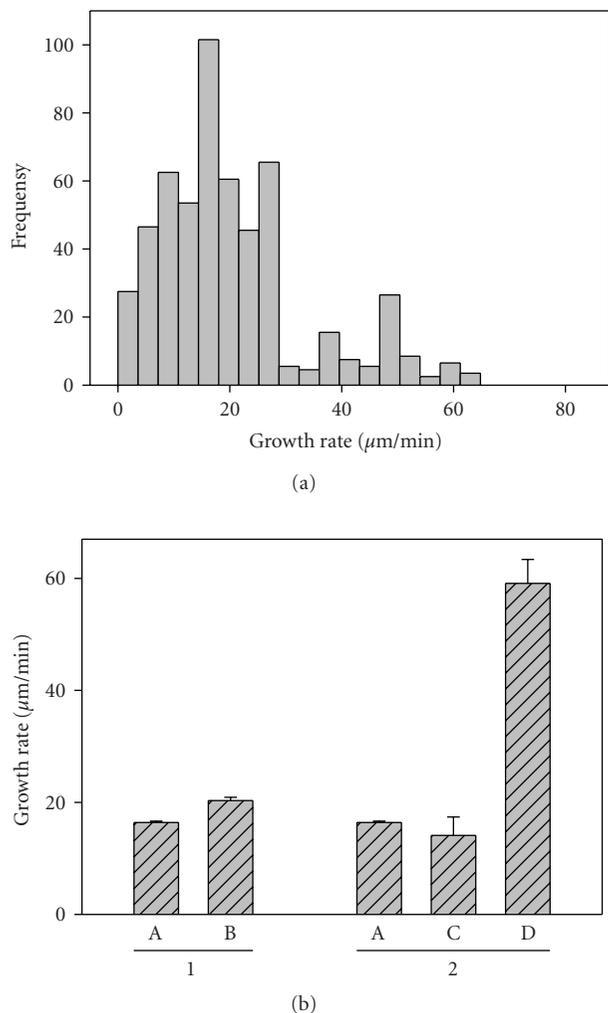
(a)

(b)

FIGURE 4: Microtubule plus-ends growth rate differences in the centrosome region of single cells and cells growing in monolayer. Growing microtubule plus-ends were selectively marked in human EC. HPAEC were transfected with the plasmid expressing EB3-GFP. Persistent microtubule growth was confirmed by long EB3-GFP tracks. EB3-GFP movement was analyzed by time-lapse microscopy. Images were acquired every 1 second. Histogram of microtubule growth rate distribution was obtained by tracking EB3-GFP comets on microtubule tips growing radially from the centrosome region in single human EC (mean growth rate, $20.6 \pm 0.6 \, \mu$m/min ($n = 72$)) (a). Mean growth rates of microtubule plus-ends in the centrosome region of cells growing in monolayer (A) and in single cells (B); mean growth rates of "normal" (C) and "fast" (D) microtubule plus-ends in single cells (b).

4. Discussion

4.1. Endothelial Microtubules Are Highly Dynamic in the Internal Cytoplasm. Our results demonstrate (Figure 1) that microtubules are highly dynamic structures in human EC. Their nonstatic plus-ends are located near the cell edge, whereas acetylated stable microtubules (~1/3 of dynamic microtubules population) are found exclusively in the central part of the cell and their plus-ends are distant from the cell edge (Table 1).

These data suggest that exactly the same dynamic microtubules may interact with the cell-cell adhesion machinery in human EC, as it was shown previously for fibroblasts [26] and epithelial cells, where microtubules are responsible for the biogenesis and turnover of the cell junctions [27–31]. Similarly to those cell types, microtubule dynamics may be involved in the regulation of cell-cell AJs to control EC specific functions, in particular, barrier permeability maintenance. However, to prove this hypothesis, we will need to perform special studies using the substances affecting the integrity of the endothelial monolayer and our EC model expressing EB3-GFP.

HPAEC expressing the GFP fusion protein specific for microtubule plus-ends were indispensable in acquiring the parameters of microtubule dynamics in real time. We were able to measure microtubule growth in the internal cytoplasm, near the centrosome, and at the periphery of human EC (Figure 2). Microtubule growth rates determined using EB3-GFP (or some others) plus-end tracking proteins are higher than those measured using fluorescein-labeled tubulin [36, 37]. This difference was observed because EB3-GFP labeled only growing microtubules. EB3 was shown to present at microtubule plus-ends during growth phases but disappeared within 5 seconds after the transition from growth to pause or shortening phase [36]. Slight pauses in the microtubule growth may be included in the measurement of microtubule growth rate calculated using fluorescein-labeled tubulin approach, thus reducing the apparent growth rate. Therefore, to avoid any discrepancy, we compared our results with published data obtained using similar approach only.

Dynamic instability behavior of microtubules is cell-type-specific [38–44] and growth rates are generally dissimilar in different cell types and in different cell areas. In hippocampal culture, the average velocity of EB3-GFP ($\approx 13 \, \mu$m/min) is no different in the cell body, the neuritis, or in the growth cone, but it is twice as high in the glia and in COS-1 cells [34]. However, early studies of microtubule behavior in living cells were limited in the cell interior but not near the cell periphery, where individual microtubule ends could be detected and their dynamics could be quantified. More recently, it has become clear that a complete understanding of microtubule behavior requires knowledge of events in the central cytoplasm and in the internal cytoplasm [36, 45].

Our data of direct quantification of microtubule dynamics in EC, obtained for the first time, clearly demonstrated (Figure 3) that the growth rates in EC are comparable with those obtained for epithelial cells and fibroblasts [36, 37]. Indeed, quantitative analysis of microtubule dynamics showed that in the case of EB3-GFP (or another plus-end tracking proteins) labeling the instantaneous rates measured in the internal cytoplasm of CHO fibroblasts was about 16-17 μm/min [36]. This was similar to that which we calculated for HPAEC (Figure 3, Table 2). Unexpectedly, our data are comparable with the rates determined for epithelial LLCPK1 cells and for CHO fibroblasts polarized and migrating directionally into the wound. The instantaneous rate of microtubule growth was similar for microtubules extending

toward the front and rear of the cell: in LLCPK1 cells the average growth rates were $17.9 \pm 7.7 \, \mu$m/min in the leading edge and $19.0 \pm 8.8 \, \mu$m/min the trailing edge, in CHO cells—16.0 ± 6.8 and $17.2 \pm 7.7 \, \mu$m/min, respectively [37]. Thus, microtubule plus-ends are highly dynamic in the internal cytoplasm of EC, and their growth rate is comparable with microtubule growth rate in fibroblasts or in functionally active cytoplasm areas in polarized and migrating cells.

4.2. Microtubule Growth Rate Varies in Different Regions of Human EC and Decreases with Monolayer Formation. The data we obtained (Figure 3) showed that the microtubule plus-end growth rate was reduced from the cell center to the cell periphery, indicating that the microtubule dynamics varied in different regions of human EC. On the other hand, microtubule growth rate was lower in EC cultivated in the monolayer than in single cells (Figure 4), and it may well be that microtubule plus-ends growth rate decreased with EC monolayer formation. Study of microtubule dynamics in living newt lung epithelial cells showed that microtubules in the extending lamellae at the leading edge are dynamic, whereas microtubules in lamellae that contact neighboring cells can be either dynamic or stable [46]. Our data (Figure 4) make it clear that in the centrosome region there are similar peculiarities in microtubule plus-ends behavior.

It was shown that in polarized, motile cells, microtubules extended into newly formed protrusions at the leading edge. These "pioneering" microtubules [47] demonstrated different behavior when compared with microtubules in nonleading, lateral edges, indicating the region-specific differences in microtubule dynamics. It is possible to assume, that the microtubules with "fast" episodes of growth which we detected in the centrosome region of single EC (Figure 4(b)) are analogues of such "pioneering" microtubules. Therefore, microtubule plus-ends behavior is different in the centrosome region and on the periphery of EC. Taken together, our results suggest the existence of different mechanisms of local regulation of microtubule plus ends elongation in EC.

The microtubule cytoskeleton is a major determinant of cortical dynamics and microtubules can interact with the cortices of animal cells in a variety of ways. One such interaction involves microtubule plus-ends, which are commonly oriented towards the cell periphery [25, 48]. Because of dynamic instability allows these plus ends may grow outwards and potentially explore peripheral structures [24], including integrin-based focal adhesions [16] and organize vesicular transport to the cell surface [49], as well as the delivery of regulatory molecules to the cortex [50].

Our findings suggest that microtubules in human EC are dynamic, with high growth rate comparable to microtubule growth rate in fibroblasts in the cell interior and lower growth rate near the cell boundary in the area of cell contacts (Figure 4). We suggest that high microtubule dynamics and local distinctions in microtubule growth rate underlie the specific function of EC where fast delivery of molecular signals to the cell edge (to the area of cell-cell junctions) is urgent for their active and fast local regulation in response to external and internal signals. Rapid growth allows nascent microtubules to elongate from the centrosome area to the cell

boundary in a very short time. Potential mechanism of high growth rate of these microtubules can be realized via their selective and more stable binding to the plus-end protein(s). This efficient association with the plus-end protein(s) may support an efficient capture of tubulin molecules or enhancing lateral interactions between individual protofilaments. The proteins of EB family (EB1 and EB3) may be involved in this process, since they control persistent microtubule growth and possess anticatastrophe activity in the cell [51].

In the EC monolayer, where AJ contacts are organized, microtubules may interact with AJs and this interaction may lead to their stabilization in the area of the contact. Cell-cell contact in lung epithelial cells was reported to stabilize the dynamic behavior of microtubule plus-ends [32, 46]. According to our results, dynamic microtubules are capable of adjusting existing contacts and can adjust endothelial permeability.
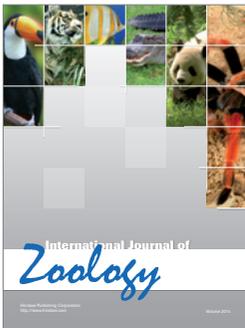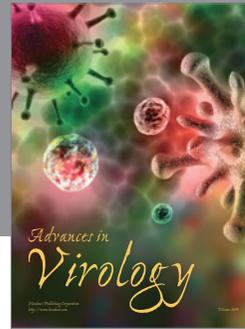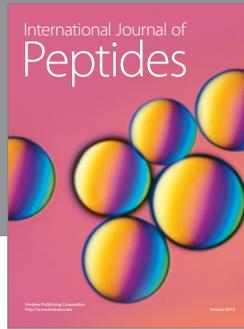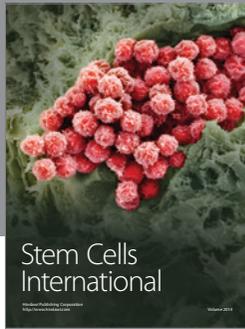
References

[1] J. G. N. Garcia, H. W. Davis, and C. E. Patterson, "Regulation of endothelial cell gap formation and barrier dysfunction: role of myosin light chain phosphorylation," *Journal of Cellular Physiology*, vol. 163, no. 3, pp. 510–522, 1995.

[2] J. G. N. Garcia, A. D. Verin, and K. L. Schaphorst, "Regulation of thrombin-mediated endothelial cell contraction and permeability," *Seminars in Thrombosis and Hemostasis*, vol. 22, no. 4, pp. 309–315, 1996.

[3] H. Lum and A. B. Malik, "Mechanisms of increased endothelial permeability," *Canadian Journal of Physiology and Pharmacology*, vol. 74, no. 7, pp. 787–800, 1996.

[4] G. P. van Nieuw Amerongen, S. van Delft, M. A. Vermeer, J. G. Collard, and V. W. M. van Hinsbergh, "Activation of rhoa by thrombin in endothelial hyperpermeability: role of rho kinase and protein tyrosine kinases," *Circulation Research*, vol. 87, no. 4, pp. 335–340, 2000.

[5] S. M. Dudek and J. G. N. Garcia, "Cytoskeletal regulation of pulmonary vascular permeability," *Journal of Applied Physiology*, vol. 91, no. 4, pp. 1487–1500, 2001.

[6] A. B. J. Groeneveld, "Vascular pharmacology of acute lung injury and acute respiratory distress syndrome," *Vascular Pharmacology*, vol. 39, no. 4-5, pp. 247–256, 2002.

[7] N. V. Bogatcheva, J. G. Garcia, and A. D. Verin, "Molecular mechanisms of thrombin-induced endothelial cell permeability," *Biochemistry*, vol. 67, no. 1, pp. 75–84, 2002.

[8] A. A. Birukova, K. G. Birukov, K. Smurova, et al., "Novel role of microtubules in thrombin-induced endothelial barrier dysfunction," *FASEB Journal*, vol. 18, no. 15, pp. 1879–1890, 2004.

[9] A. A. Birukova, K. Smurova, K. G. Birukov, et al., "Microtubule disassembly induces cytoskeletal remodeling and lung vascular barrier dysfunction: role of Rho-dependent mechanisms," *Journal of Cellular Physiology*, vol. 201, no. 1, pp. 55–70, 2004.

[10] F. Breviario, L. Caveda, M. Corada, et al., "Functional properties of human vascular endothelial cadherin (7B4/cadherin-5), an endothelium-specific cadherin," *Arteriosclerosis, Thrombosis, and Vascular Biology*, vol. 15, no. 8, pp. 1229–1239, 1995.

[11] E. Dejana, G. Bazzoni, and M. G. Lampugnani, "Vascular endothelial (VE)-cadherin: only an intercellular glue?" *Experimental Cell Research*, vol. 252, no. 1, pp. 13–19, 1999.

[12] D. Mehta and A. B. Malik, "Signaling mechanisms regulating endothelial permeability," *Physiological Reviews*, vol. 86, no. 1, pp. 279–367, 2006.

[13] D. Vestweber, "Adhesion and signaling molecules controlling the transmigration of leukocytes through endothelium," *Immunological Reviews*, vol. 218, no. 1, pp. 178–196, 2007.

[14] E. Vandenbroucke, D. Mehta, R. Minshall, and A. B. Malik, "Regulation of endothelial junctional permeability," *Annals of the New York Academy of Sciences*, vol. 1123, pp. 134–145, 2008.

[15] J. V. Small, B. Geiger, I. Kaverina, and A. Bershadsky, "How do microtubules guide migrating cells?" *Nature Reviews Molecular Cell Biology*, vol. 3, no. 12, pp. 957–964, 2002.

[16] J. V. Small and I. Kaverina, "Microtubules meet substrate adhesions to arrange cell polarity," *Current Opinion in Cell Biology*, vol. 15, no. 1, pp. 40–47, 2003.

[17] A. D. Bershadsky, N. Q. Balaban, and B. Geiger, "Adhesion-dependent cell mechanosensitivity," *Annual Review of Cell and Developmental Biology*, vol. 19, pp. 677–695, 2003.

[18] A. D. Bershadsky, C. Ballestrem, L. Carramusa, et al., "Assembly and mechanosensory function of focal adhesions: experiments and models," *European Journal of Cell Biology*, vol. 85, no. 3-4, pp. 165–173, 2006.

[19] J. M. Schober, Y. A. Komarova, O. Y. Chaga, A. Akhmanova, and G. G. Borisy, "Microtubule-targeting-dependent reorganization of filodopia," *Journal of Cell Science*, vol. 120, no. 7, pp. 1235–1244, 2007.

[20] M. Prager-Khoutorsky, I. Goncharov, A. Rabinkov, D. Mirelman, B. Geiger, and A. D. Bershadsky, "Allicin inhibits cell polarization, migration and division via its direct effect on microtubules," *Cell Motility and the Cytoskeleton*, vol. 64, no. 5, pp. 321–337, 2007.

[21] A. Efimov, A. Kharitonov, N. Efimova, et al., "Asymmetric CLASP-dependent nucleation of noncentrosomal microtubules at the trans-Golgi network," *Developmental Cell*, vol. 12, no. 6, pp. 917–930, 2007.

[22] J. A. Broussard, D. J. Webb, and I. Kaverina, "Asymmetric focal adhesion disassembly in motile cells," *Current Opinion in Cell Biology*, vol. 20, no. 1, pp. 85–90, 2008.

[23] M. Moritz and D. A. Agard, "γ-tubulin complexes and microtubule nucleation," *Current Opinion in Structural Biology*, vol. 11, no. 2, pp. 174–181, 2001.

[24] J. Howard and A. A. Hyman, "Dynamics and mechanics of the microtubule plus end," *Nature*, vol. 422, no. 6933, pp. 753–758, 2003.

[25] A. Akhmanova and C. C. Hoogenraad, "Microtubule plus-end-tracking proteins: mechanisms and functions," *Current Opinion in Cell Biology*, vol. 17, no. 1, pp. 47–54, 2005.

[26] S. Mary, S. Charrasse, M. Meriane, et al., "Biogenesis of N-cadherin-dependent cell-cell contacts in living fibroblasts is a microtubule-dependent kinesin-driven mechanism," *Molecular Biology of the Cell*, vol. 13, no. 1, pp. 285–301, 2002.

[27] A. M. Shewan, M. Maddugoda, A. Kraemer, et al., "Myosin 2 is a key Rho kinase target necessary for the local concentration of E-cadherin at cell-cell contacts," *Molecular Biology of the Cell*, vol. 16, no. 10, pp. 4531–4542, 2005.

[28] R. Vogelmann and W. J. Nelson, "Fractionation of the epithelial apical junctional complex: reassessment of protein distributions in different substructures," *Molecular Biology of the Cell*, vol. 16, no. 2, pp. 701–716, 2005.

[29] L. Carramusa, C. Ballestrem, Y. Zilberman, and A. D. Bershadsky, "Mammalian diaphanous-related formin Dia1 controls the organization of E-cadherin-mediated cell-cell junctions," *Journal of Cell Science*, vol. 120, no. 21, pp. 3870–3882, 2007.

[30] W. Meng, Y. Mushika, T. Ichii, and M. Takeichi, "Anchorage of microtubule minus ends to adherens junctions regulates epithelial cell-cell contacts," *Cell*, vol. 135, no. 5, pp. 948–959, 2008.

[31] A. Akhmanova, S. J. Stehbens, and A. S. Yap, "Touch, grasp, deliver and control: functional cross-talk between microtubules and cell adhesions," *Traffic*, vol. 10, no. 3, pp. 268–274, 2009.

[32] S. J. Stehbens, A. D. Paterson, M. S. Crampton, et al., "Dynamic microtubules regulate the local concentration of E-cadherin at cell-cell contacts," *Journal of Cell Science*, vol. 119, no. 9, pp. 1801–1811, 2006.

[33] K. M. Smurova, A. A. Birukova, A. D. Verin, and I. B. Alieva, "The microtubule system in endothelial barrier dysfunction: disassembly of peripheral microtubules and microtubules reorganization in internal cytoplasm," *Tsitologiya*, vol. 50, no. 1, pp. 49–55, 2008.

[34] T. Stepanova, J. Slemmer, C. C. Hoogenraad, et al., "Visualization of microtubule growth in cultured neurons via the use of EB3-GFP (end-binding protein 3-green fluorescent protein)," *Journal of Neuroscience*, vol. 23, no. 7, pp. 2655–2664, 2003.

[35] J. C. Bulinski and G. G. Gundersen, "Stabilization and post-translational modification of microtubules during cellular morphogenesis," *BioEssays*, vol. 13, no. 6, pp. 285–293, 1991.

[36] Y. A. Komarova, I. A. Vorobjev, and G. G. Borisy, "Life cycle of MTs: persistent growth in the cell interior, asymmetric transition frequencies and effects of the cell boundary," *Journal of Cell Science*, vol. 115, no. 17, pp. 3527–3539, 2002.

[37] K. J. Salaycik, C. J. Fagerstrom, K. Murthy, U. S. Tulu, and P. Wadsworth, "Quantification of microtubule nucleation, growth and dynamics in wound-edge cells," *Journal of Cell Science*, vol. 118, no. 18, pp. 4113–4122, 2005.

[38] E. Schulze and M. Kirschner, "Microtubule dynamics in interphase cells," *Journal of Cell Biology*, vol. 102, no. 3, pp. 1020–1031, 1986.

[39] E. Schulze and M. Kirschner, "Dynamic and stable populations of microtubules in cells," *Journal of Cell Biology*, vol. 104, no. 2, pp. 277–288, 1987.

[40] P. J. Sammak and G. G. Borisy, "Direct observation of microtubule dynamics in living cells," *Nature*, vol. 332, no. 6166, pp. 724–726, 1988.

[41] L. Cassimeris, "Regulation of microtubule dynamic instability," *Cell Motility and the Cytoskeleton*, vol. 26, no. 4, pp. 275–281, 1993.

[42] E. Shelden and P. Wadsworth, "Observation and quantification of individual microtubule behavior in vivo: microtubule dynamics are cell-type specific," *Journal of Cell Biology*, vol. 120, no. 4, pp. 935–945, 1993.

[43] A. Akhmanova, C. C. Hoogenraad, K. Drabek, et al., "CLASPs are CLIP-115 and -170 associating proteins involved in the regional regulation of microtubule dynamics in motile fibroblasts," *Cell*, vol. 104, no. 6, pp. 923–935, 2001.

[44] P. S. Vaughan, P. Miura, M. Henderson, B. Byrne, and K. T. Vaughan, "A role for regulated binding of p150(Glued) to microtubule plus ends in organelle transport," *Journal of Cell Biology*, vol. 158, no. 2, pp. 305–319, 2002.

[45] I. A. Vorobjev, I. B. Alieva, I. S. Grigoriev, and G. G. Borisy, "Microtubule dynamics in living cells: direct analysis in the internal cytoplasm," *Cell Biology International*, vol. 27, no. 3, pp. 293–294, 2003.

[46] C. M. Waterman-Storer, W. C. Salmon, and E. D. Salmon, "Feedback interactions between cell-cell adherens junctions and cytoskeletal dynamics in newt lung epithelial cells," *Molecular Biology of the Cell*, vol. 11, no. 7, pp. 2471–2483, 2000.

[47] C. M. Waterman-Storer and E. D. Salmon, "Actomyosin-based retrograde flow of microtubules in the lamella of migrating epithelial cells influences microtubule dynamic instability and turnover and is associated with microtubule breakage and treadmilling," *Journal of Cell Biology*, vol. 139, no. 2, pp. 417–434, 1997.

[48] G. G. Gundersen, E. R. Gomes, and Y. Wen, "Cortical control of microtubule stability and polarization," *Current Opinion in Cell Biology*, vol. 16, no. 1, pp. 106–112, 2004.

[49] T. Watanabe, J. Noritake, and K. Kaibuchi, "Regulation of microtubules in cell migration," *Trends in Cell Biology*, vol. 15, no. 2, pp. 76–83, 2005.

[50] O. C. Rodriguez, A. W. Schaefer, C. A. Mandato, P. Forscher, W. M. Bement, and C. M. Waterman-Storer, "Conserved microtubule-actin interactions in cell movement and morphogenesis," *Nature Cell Biology*, vol. 5, no. 7, pp. 599–609, 2003.

[51] Y. Komarova, C. O. De Groot, I. Grigoriev, et al., "Mammalian end binding proteins control persistent microtubule growth," *Journal of Cell Biology*, vol. 184, no. 5, pp. 691–706, 2009.

BioMed
Research International

Stem Cells
International

International Journal of
Peptides

Advances in
Virology

International Journal of
Genomics

International Journal of
Zoology

Journal of
Nucleic Acids

Journal of
Signal Transduction

Hindawi

Submit your manuscripts at
http://www.hindawi.com

The Scientific
World Journal

Genetics
Research International

Anatomy
Research International

International Journal of
Microbiology

Biochemistry
Research International

Advances in
Bioinformatics

Archaea

Enzyme
Research

International Journal of
Evolutionary Biology

Molecular Biology
International

Journal of
Marine Biology